Supporting Information

Optimization of structural expansion and contraction for TiS_2 by controlling the electrochemical window of intercalation/delithiation

Xue Han[a], Min Wang[a], Jingxian Yu[b], Shengping Wang[a,*]

[a] Faculty of Materials Science and Chemistry, China University of Geosciences, Wuhan 430074, China

[b] ARC Centre of Excellence for Nanoscale BioPhotonics (CNBP), School of Chemistry and Physics, The University of Adelaide, Adelaide, SA 5005, Australia

* Corresponding Author. spwang@cug.edu.cn

Experimental methods

i. Synthesis of TiS_2

In an Ar atmosphere, 800 mg sulfur was dissolved in 25 mL oleylamine and stirred at 100 °C for 0.5 h. Then, 2 mL $TiCl_4$ was added to the solution, which was heated to 300 °C at 10 °C min^{-1}, and the solution was kept at 300 °C for 3 h. The product was collected by centrifugation and washed several times with cyclohexane and ethanol. Finally, TiS_2 samples were obtained after heating at 400 °C for 2 h in an Ar atmosphere.

ii. General characterization

The X-ray diffraction (XRD) patterns were collected on a Bruker D8 Focus powder diffractometer with Cu Kα radiation. The experimental patterns were refined by the Rietveld method using GSAS software and the EXPGUI interface [1].

The morphology of the materials was observed with field emission scanning electron microscopy (FESEM) on an SU8010, and the morphology and structures were also captured and analyzed with transmission electron microscopy (TEM) on a Philips CM12 at 200 kV equipped with selected area electron diffraction (SAED).

iii. Preparation of the test batteries

The working electrodes were prepared by casting a well-homogenized slurry that contained TiS_2 (75 wt%), acetylene black (15 wt%), and polyvinylidene fluoride (10 wt%) in N-methyl-2-pyrrolidone on one side of a copper foil. After solvent evaporation, the electrodes were cut into discs with diameters of 10 mm and dried thoroughly in a vacuum oven at 80 °C for 24 h. The mass loading of TiS_2 on an electrode was 1.5 mg cm^{-2}.

All 2016-type coin batteries for the electrochemical measurements were assembled in an argon-filled glove box with oxygen and moisture levels below 0.5 ppm. Metal lithium foils (15 mm diameter and 0.3 mm thickness) served as the counter electrode, a Celgard 2400 microporous membrane served as the separator, and 1 M lithium bis(trifluoromethylsulfonyl)imide in a mixture of 1,3-dioxane and dimethoxyethane with a volume ratio of 1:1 served as the electrolyte. Then, 0.3 mL electrolyte was added into a test battery.

iv. Electrochemical measurements

The galvanostatic discharge/charge (GDC) and differential capacitance (dQ/dV) curves of the batteries were tested on a BT2000 Arbin battery test system at various current densities. The cyclic voltammetry (CV), galvanostatic intermittent titration (GITT), and electrochemical impedance spectroscopy (EIS) were carried out using a Bio-Logic VMP3 multichannel electrochemical workstation.

The CV curves at a scan rate of 0.1 mV s^{-1} with various potential ranges were recorded. GITT experiments were conducted over the potential range from the open-circuit voltage (OCV) to 0.01 V at a current density of 0.3 mA cm^{-2} with a constant current pulse for 10 min and a relaxation time of 180 min. EIS was performed with a disturbance amplitude of 5 mV in a frequency range from 100 kHz to 10 mHz.

The test batteries for EIS had a current of 96 mA g^{-1} from the OCV to 0.01 V and a current of 96 mA g^{-1} from 0.01 V to 2.8 V. The EIS tests were conducted with capacity steps of 96 mAh g^{-1}. The other test batteries for EIS had 5 cycles at 0.1 mA cm^{-2} from 0.9 (or 0.8) V to 2.8 V, and EIS was recorded at 0.9 (or 0.8) V for the low cutoff potential and 2.8 V for the high cutoff potential. At each test point, the batteries were held for 2 h to achieve charge equilibrium.

The test batteries were kept at 25 °C during the experiments. The calculation of the capacity density was based on the mass of the loaded TiS_2.

v. Computational details.

The geometries of Li_xTiS_2 (x = 0-3) were optimized using the SIESTA 4.0 package, [2] which employs norm-conserving pseudopotentials. Structural relaxation allows both atomic coordinates and cell parameters to relax. All calculations were carried out with the general gradient approximation (GGA) [3] of Perdew, Burke and Emzerhof (PBE) [4] used for all atoms in electronic structure calculations until the force on each atom was smaller than 0.02 eV/Å. The valence electronic orbitals of the systems were described using double-ζ polarized (DZP) basis sets, and a cutoff energy of 250 Ry was used. The Brillouin zone was sampled as a Monkhorst-Pack grid using 10 × 10 × 10 k-points. The optimized cell parameters of TiS_2 and $LiTiS_2$ are remarkably close to their respective values (mp-2156 and mp-1815349) obtained from the Materials Project (https://materialsproject.org/) (less than 3%), indicating a high reliability of the SIESTA approach. All of the structures were visualized by VESTA [5].

$$TiS_2 + xLi^+ \leftrightarrow Li_xTiS_2 \ (0 \le x \le 1) \tag{1}$$

$$Li_xTiS_2 + (4 - x)Li^+ + (4 - x)e^- \rightarrow Ti + 2Li_2S \tag{2}$$

$$D_{Li^+} = \frac{4}{\pi\tau}\left(\frac{mV_M}{MS}\right)^2\left(\frac{\Delta E_s}{\Delta E_t}\right)^2 \tag{3}$$

Where τ is the time for an applied galvanostatic current; m, M, and V_M are the mass, relative molecular mass, and molar volume of TiS_2, respectively; S is the active surface of the electrode (taken as the geometric area of the electrode); and ΔE_s and ΔE_t are the quasi-equilibrium potential and the change in the battery potential E during the current pulse, respectively.

$$i = av^b \tag{4}$$

$$logi = b \times logv + loga \tag{5}$$

$$i = k_1v + k_2v^{\frac{1}{2}} \tag{6}$$

$$\frac{i}{v^{\frac{1}{2}}} = k_1v^{\frac{1}{2}} + k_2 \tag{7}$$

Where i is the peak current (mA), v is the scanning speed (mV s^{-1}), and a and b are adjustable parameters. Generally, the electrochemical reaction with b of 0.5 was a charge storage process dominated by diffusion control, and the electrochemical reaction with b of 1.0 was a charge storage process dominated by capacitive behavior [6]. When b was 0.5-1.0, it was considered that both the diffusion and capacitance behaviors dominated the charge storage process.

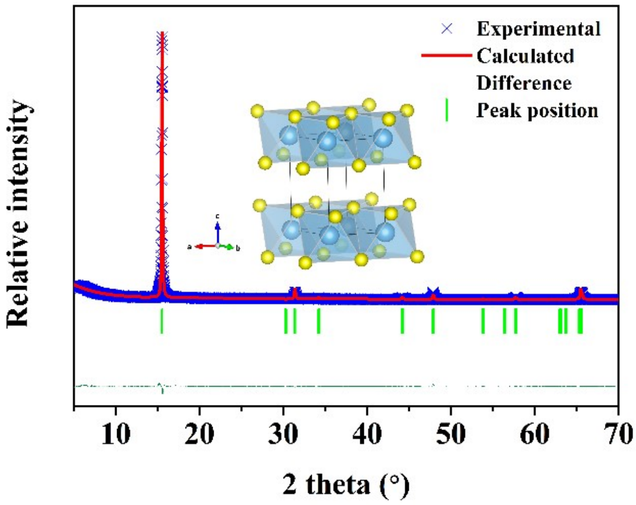

Formula	TiS_2
Symmetry	Trigonal system
Space group	P -3m 1
Cell parameters	$a = b = 3.41$ Å; $c = 5.70$ Å; $\alpha = \beta = 90°$; $\gamma = 120°$ $V = 57.29$ Å^3
R_{wp}	11.6%
R_p	8.2 %

Fig. S1 Refined XRD patterns and the simulated results of TiS_2.

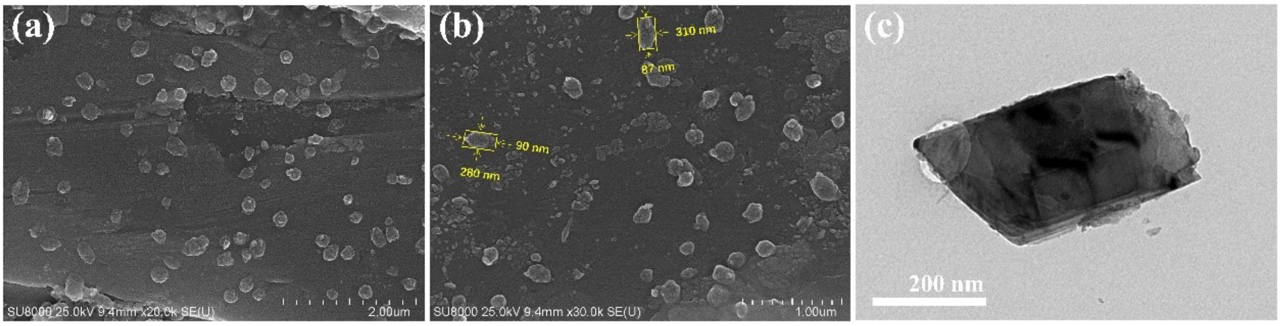

Fig. S2 SEM (a, b) and TEM (c) images for TiS_2.

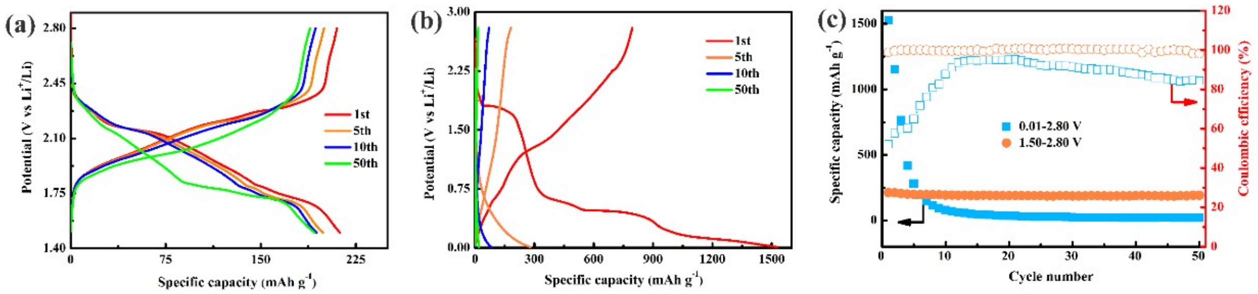

Fig. S3 Discharge/charge curves and cycle performance of TiS_2 at 0.1 mA cm^{-2} with 1.50-2.80 V (a, c) and 0.01-2.80 V (b, c).

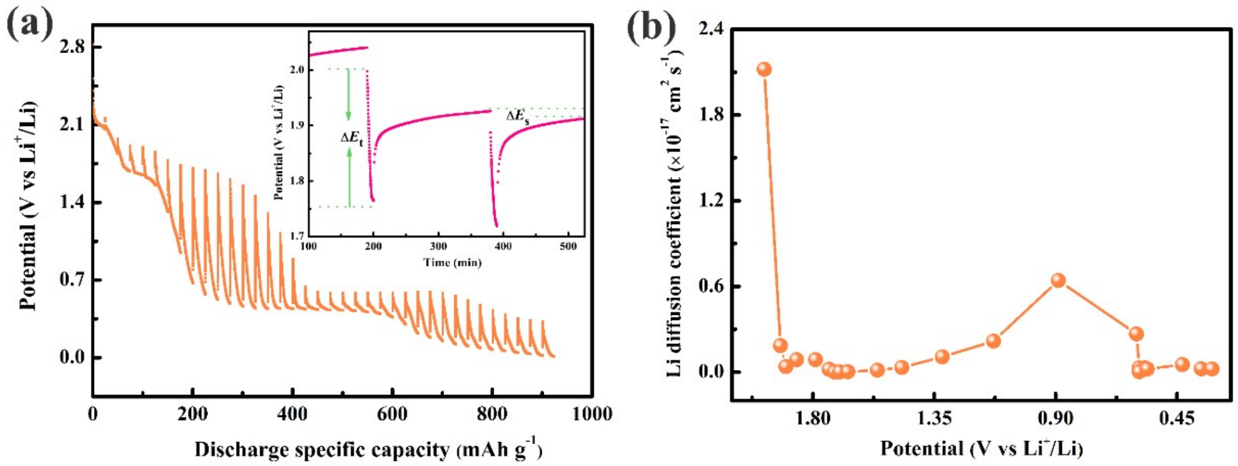

Fig. S4 Discharge curve and GITT curves (a) and lithium ion diffusion coefficients (b) of TiS_2

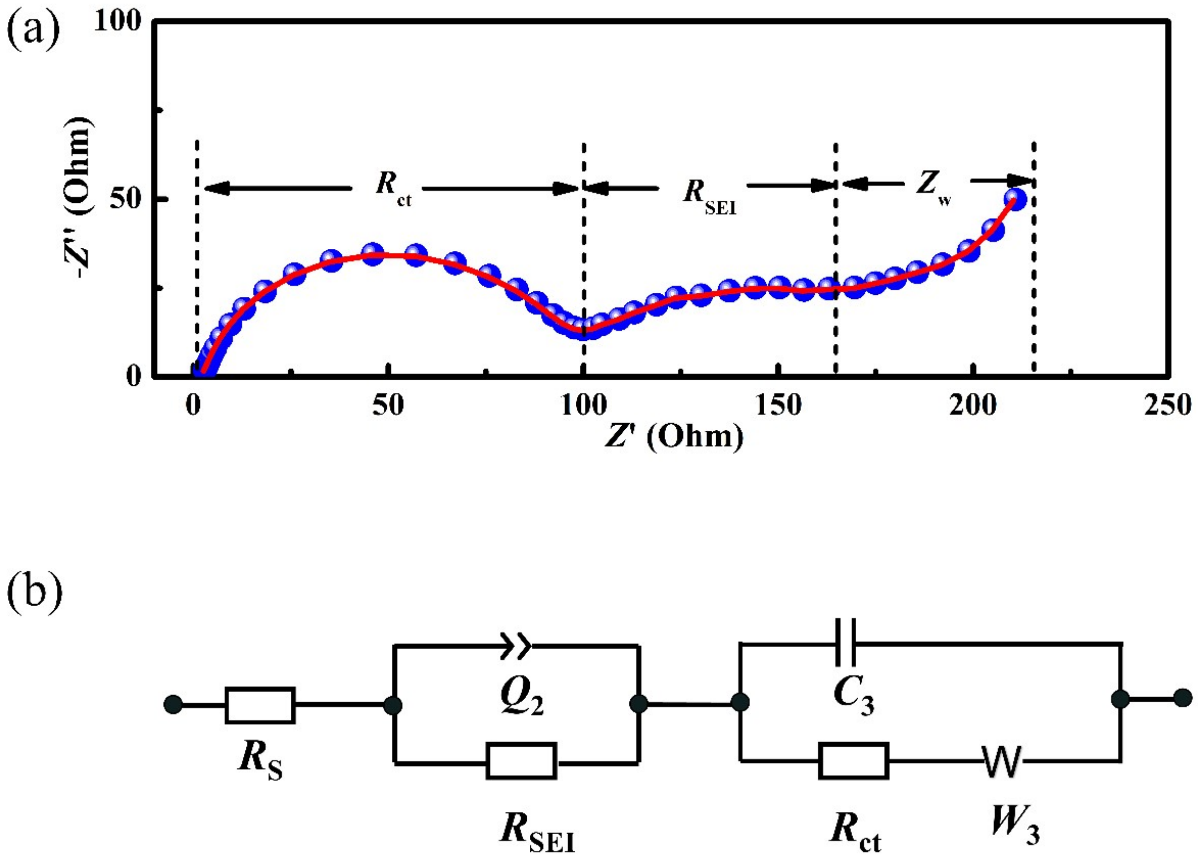

Fig. S5 EIS (a) and equivalent circuit diagram (b) of TiS_2 with discharge to 0.01 V, the points represent the measured data and the line represents the fitted data.

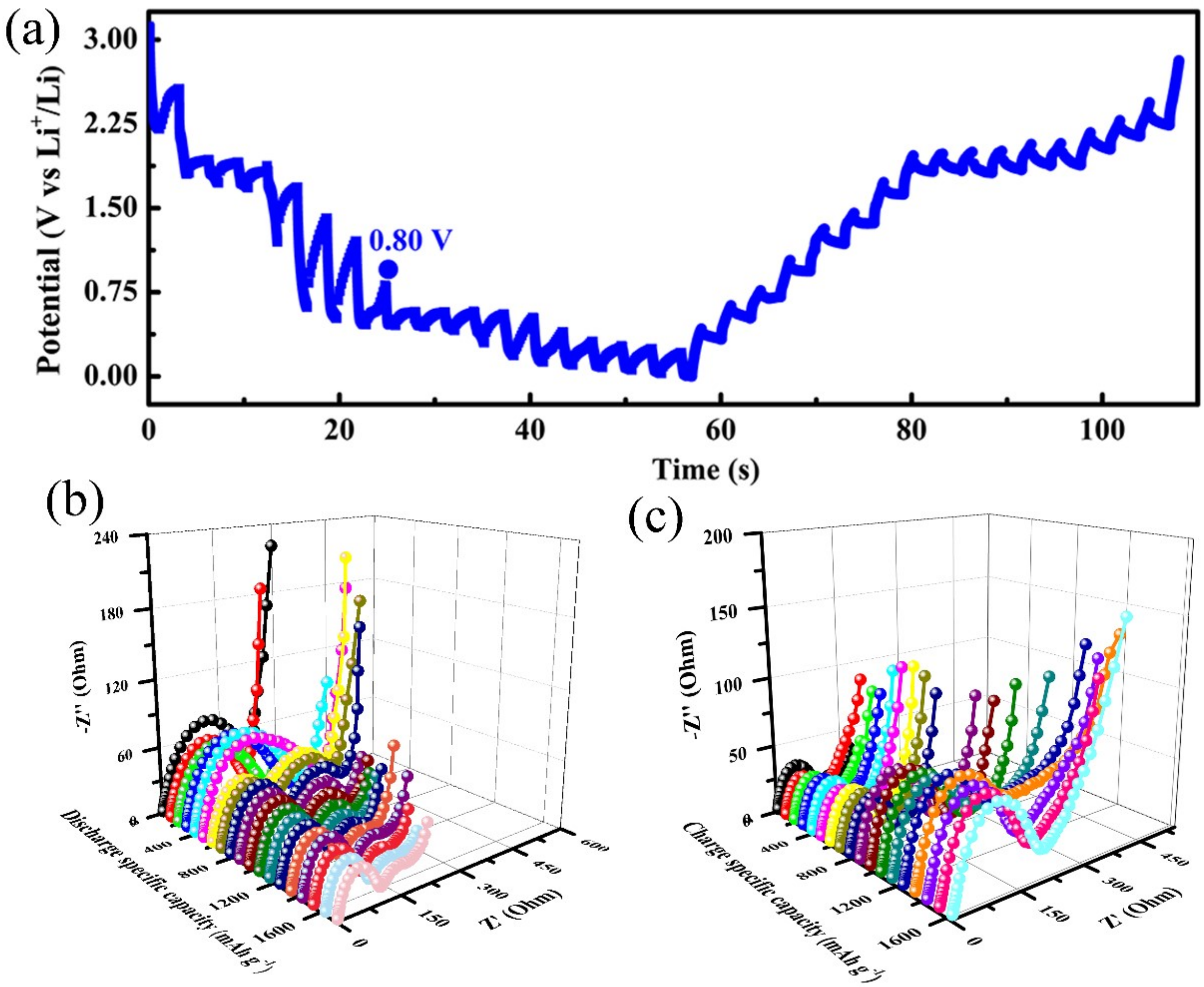

Fig. S6 First discharge/charge curves with EIS test (a), and the EIS profiles at various DODs (b) and DOCs (c) of TiS_2.

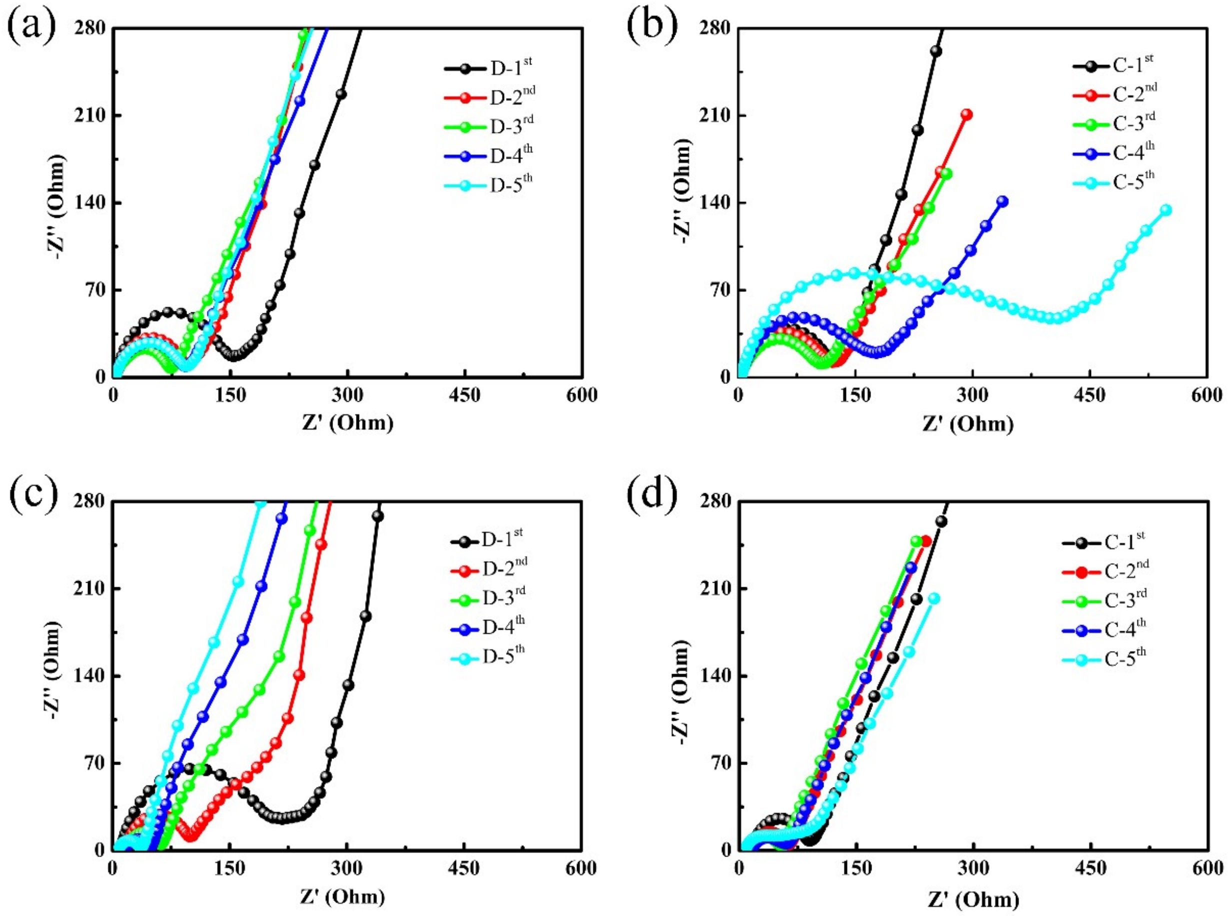

Fig. S7 EIS profiles of TiS_2 at full states of discharge/charge for various cycles with 0.80-2.80 V (a, b) and 0.90-2.80 V (c, d).

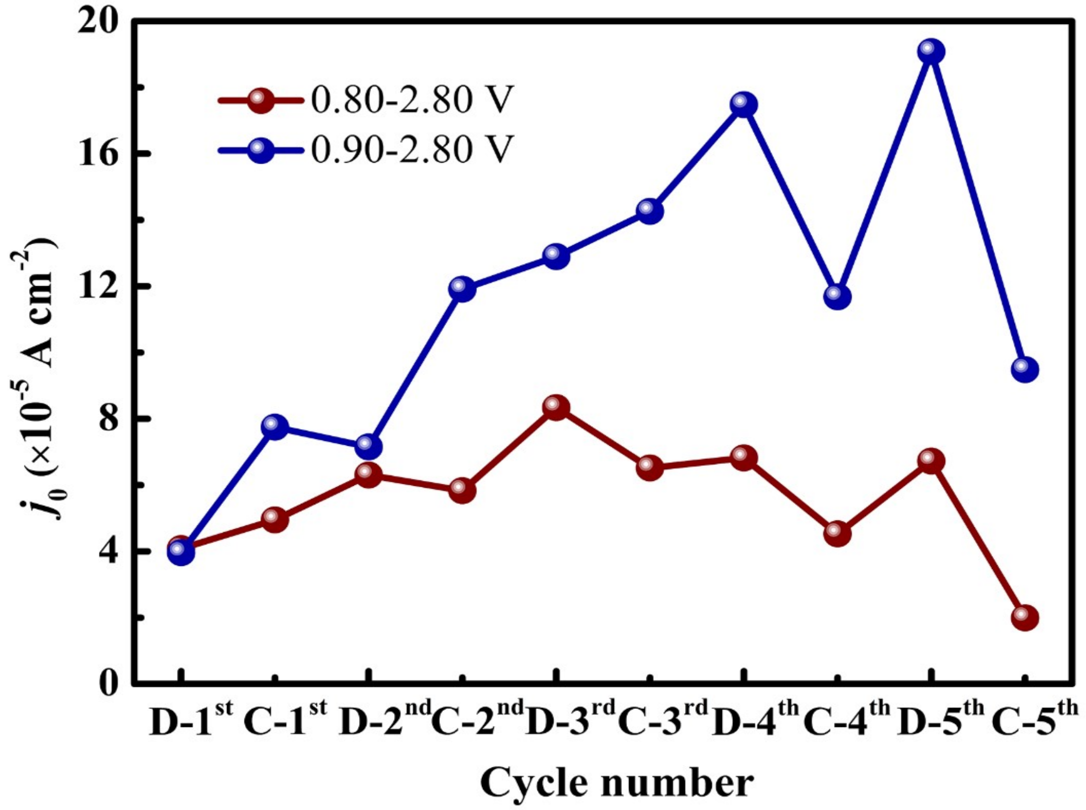

Fig. S8 Exchange current density of TiS_2 at full states of discharge/charge for various cycles with 0.8-2.8 V and 0.9-2.8 V.

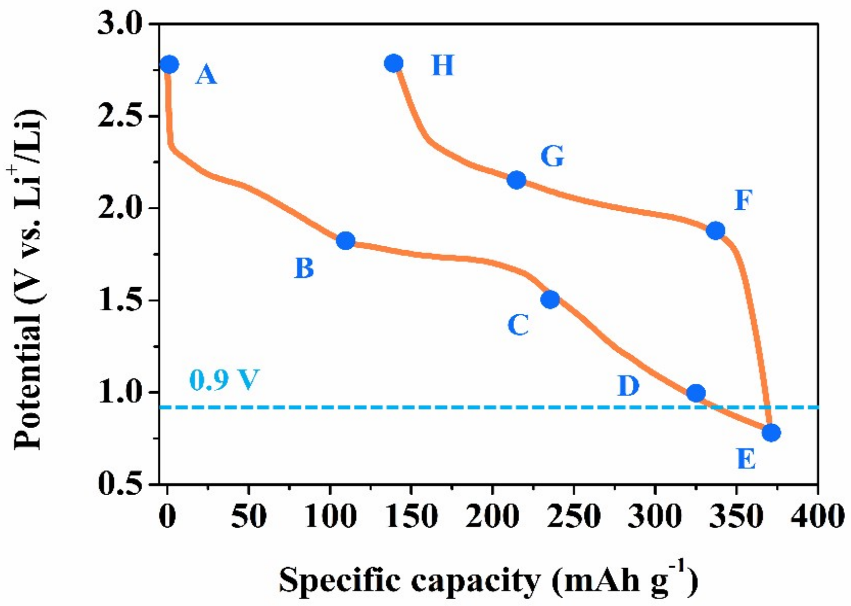

Fig. S9 Charge/discharge curve and the collected points of ex situ XRD.

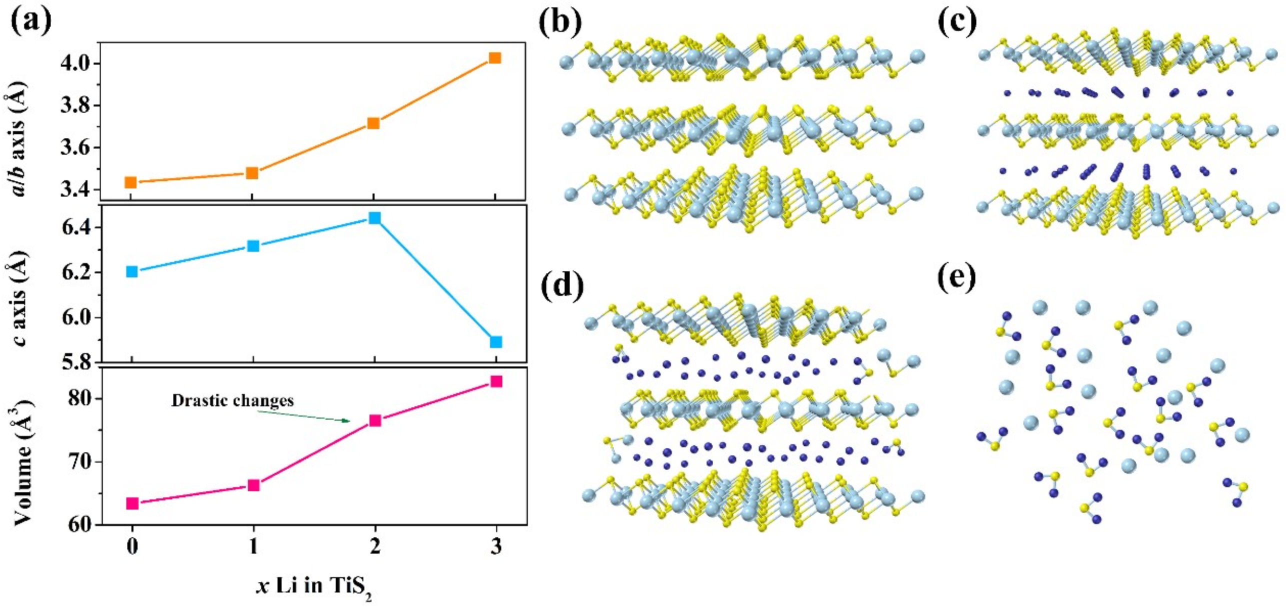

Fig. S10 The results of geometric optimization (a) for TiS_2 and the structural evolution of TiS_2 during the lithiation process for pristine state (b) and discharge to 0.9 (c), 0.8 (d), and 0.01 V (e).

Table S1 Comparison of capacity retention of TiS_2 with different cutoff voltages

Cutoff voltage of discharge	10th	50th	100th
0.8 V (This work)	**86%**	**42%**	**18%**
0.9 V (This work)	**92%**	**91%**	**88%%**
1.0 V [7]	92%	99%	100%
1.4 V [8]	92%	91%	91%
0.05 V [8]	42%	32%	33%
1.0 V [9]	100%	100%	
1.5 V [10]	100%	100%	
1.5 V [11]	97%	94%	

References

1. B.H. Toby, EXPGUI, a graphical user interface for GSAS, *J. Appl. Crystallogr.*, 2001, 34, 210-213. https://doi.org/10.1107/S0021889801002242
2. J.M. Soler, E. Artacho, J.D. Gale, A. García, J. Junquera, P. Ordejón, D. Sánchez-Portal, The SIESTA method for ab initio order-N materials simulation, *J. Phys.: Condens. Matter*, 2002, 14, 2745. https://doi.org/10.1088/0953-8984/14/11/302
3. J.P. Perdew, K. Burke, M. Ernzerhof, Generalized gradient approximation made simple, *Phys. Rev. Lett.*, 1996, 77, 3865-3868. https://doi.org/10.1103/PhysRevLett.77.3865
4. B. Hammer, L.B. Hansen, J.K. Nørskov, Improved adsorption energetics within density-functional theory using revised Perdew-Burke-Ernzerhof functionals, *Phys. Rev. B*, 1999, 59, 7413-7421. https://doi.org/10.1103/PhysRevB.59.7413
5. K. Momma, F. Izumi, VESTA: a three-dimensional visualization system for electronic and structural analysis, *J. Appl. Crystallogr.*, 2008, 41, 653-658. https://doi.org/10.1107/S0021889808012016
6. H.-S. Kim, J.B. Cook, H. Lin, J.S. Ko, S.H. Tolbert, V. Ozolins, B. Dunn, Oxygen vacancies enhance pseudocapacitive charge storage properties of MoO_{3-x}, *Nature Mater.*, 2017, 16, 454-460. https://doi.org/10.1038/nmat4810
7. P. Hu, B. Wang, D. Xiao, K. Aifantis, Capturing the differences between lithiation and sodiation of nanostructured TiS_2 electrodes, *Nano Energy*, 2019, 63, 103820. https://doi.org/10.1016/j.nanoen.2019.06.016
8. L. Zhang, D. Sun, J. Kang, H.-T. Wang, S.-H. Hsieh, W.-F. Pong, H.A. Bechtel, J. Feng, L.-W. Wang, E.J. Cairns, J. Guo, Tracking the chemical and structural evolution of the TiS_2 electrode in the lithium-ion cell using operando X-ray absorption spectroscopy, *Nano Lett.*, 2018, 18, 4506-4515. https://doi.org/10.1021/acs.nanolett.8b01680
9. D.Y. Oh, Y.E. Choi, D.H. Kim, Y.-G. Lee, B.S. Kim, J. Park, H. Sohn, Y.S. Jung, All-solid-state lithium-ion batteries with TiS_2 nanosheets and sulphide solid electrolytes, *J. Mater. Chem. A*, 2016, 4, 10329-10335. https://doi.org/10.1039/c6ta01628f
10. B. Shin, Y.J. Nam, J.W. Kim, Y.-G. Lee, Y.S. Jung, Interfacial architecture for extra Li^+ storage in all-solid-state lithium batteries, *Sci. Rep.*, 2014, 4, 5572. https://doi.org/10.1038/srep05572
11. J.E. Trevey, C.R. Stoldt, S.-H. Lee, High power nanocomposite TiS_2 cathodes for all-solid-state lithium batteries, *J. Electrochem. Soc.*, 2011, 158, A1282-A1289. https://doi.org/10.1149/2.017112jes